

Generalized Deep Multi-view Clustering via Causal Learning with Partially Aligned Cross-view Correspondence

Xihong Yang^{1,3}, Siwei Wang², Jiaqi Jin¹, Fangdi Wang¹, Tianrui Liu¹,
 , Yueming Jin³, Xinwang Liu^{1,*}, En Zhu^{1,*}, Kunlun He⁴

¹College of Computer Science and Technology, National University of Defense Technology, Changsha, China ²Intelligent Game and Decision Lab, Beijing, China

³National University of Singapore, Singapore ⁴Chinese PLA General Hospital, Beijing, China

{yangxihong, xinwangliu, enzhu}@nudt.edu.cn

Abstract

Multi-view clustering (MVC) aims to explore the common clustering structure across multiple views. Many existing MVC methods heavily rely on the assumption of view consistency, where alignments for corresponding samples across different views are ordered in advance. However, real-world scenarios often present a challenge as only partial data is consistently aligned across different views, restricting the overall clustering performance. In this work, we consider the model performance decreasing phenomenon caused by data order shift (i.e., from fully to partially aligned) as a generalized multi-view clustering problem. To tackle this problem, we design a **causal** multi-view clustering network, termed **CauMVC**. We adopt a causal modeling approach to understand multi-view clustering procedure. To be specific, we formulate the partially aligned data as an intervention and multi-view clustering with partially aligned data as an post-intervention inference. However, obtaining invariant features directly can be challenging. Thus, we design a Variational Auto-Encoder for causal learning by incorporating an encoder from existing information to estimate the invariant features. Moreover, a decoder is designed to perform the post-intervention inference. Lastly, we design a contrastive regularizer to capture sample correlations. To the best of our knowledge, this paper is the first work to deal generalized multi-view clustering via causal learning. Empirical experiments on both fully and partially aligned data illustrate the strong generalization and effectiveness of CauMVC.

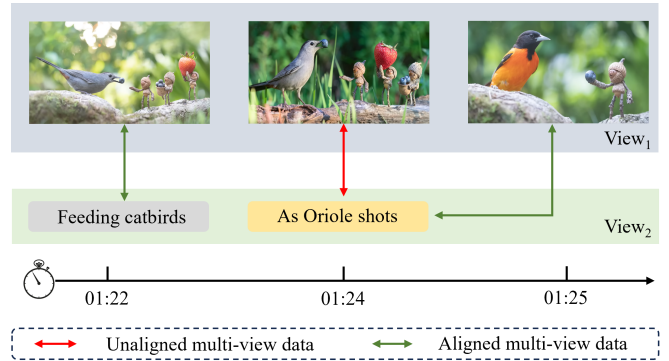


Figure 1. An illustrative example of the motivation is presented through a raw video and its corresponding description. In this example, the issue of partial alignment between the video and the description becomes evident. In this scenario, we consider the video as one view and the description as another. There is a noticeable mismatch between the description and the visual content. For instance, when the description mentions “Oriole,” the video content actually shows “feeding catbirds” at the timestamp “01:24”.

1. Introduction

Multi-view clustering (MVC) [2, 6, 8, 9, 17, 23, 39, 44–46, 54, 60, 65, 69–71, 75] is a critical task for uncovering semantic information and partitioning data into distinct groups in an unsupervised manner, gaining significant attention in recent years.

Although existing MVC algorithms demonstrate promising clustering performance, they heavily rely on the assumption that the mapping of all corresponding samples between views is ordered. This reliance facilitates learning a common representation and makes clustering feasible. However, in real application, the multi-view data is always partially aligned. To be concrete, taking a multi-view dataset $\{\mathbf{X}^1, \mathbf{X}^2\}$ as an example, the data x_i^1 and x_i^2 with the same index in two views may represent different con-

*Corresponding author

tent. The generalization and performance of MVC models diminish when erroneous alignment information between views misleads the final clustering outcome [68]. As illustrated in Fig. 1, the video content and its corresponding text description represent two distinct views. In this scenario, the text description does not synchronize with the video content¹. Recently, a serious multi-view clustering are proposed to solve this problem. MVC-UM [68] employed non-negative matrix factorization to address unknown cross-view mappings. Besides, PVC [14] utilized a differentiable surrogate for the Hungarian algorithm to establish class-level correspondences in unaligned data, while SURE [58] introduced a noise-robust contrastive loss function. Despite achieving promising clustering performance, these algorithms overlook the causality between fully aligned and partially aligned data, lacking a unified causal framework to address the partially aligned problem.

In this work, we consider the partially aligned data as the data shift. The objective is to realize strong generalization of the model. To achieve the above objective, we leverage causal method to delve into the cause-effect dynamics within the multi-view clustering process. We categorize the features into variant features x_{va} and invariant features x_{in} . Here, we consider the input raw features as the variant features since those features are different for cross-view scenario. The invariant features conflict the fundamental attributes of the data, which keep consistent in different views. Taking the example in Fig. 2 for illustration, for example, we demonstrate the variant and invariant features of a bird. Further, we classify the representations into two classes based on whether they are influenced by the variant features or not. The causal graph depicted in Fig. 4 illustrates the relationships from variant features x_{va} and invariant features x_{in} to the extracted variant representations e_{va} and invariant representations e_{in} , culminating in the clustering result r . Existing methods extract representations by encoding the original multi-view raw feature inputs, i.e., variant feature x_{va} . When the input features drift from fully aligned data x_{va} to partially aligned data x'_{va} , this paradigm will fail [14, 58]. From the causal perspective, MVC with partially aligned data is viewed as the post-intervention inference result probabilities $p(r|do(x_{va} = x'_{va}), x_{in})$, where the input shift from x_{va} to x'_{va} is formulated as intervention.

To be specific, we design a **Causal Multi-View Clustering** network to realize the strong generalization with partially aligned data, termed CauMVC. The challenge is to obtain the invariant features x_{in} essential for estimating $p(r|do(x_{va} = x'_{va}), x_{in})$. To overcome this problem, we employ a variational autoencoder (VAE) for inferring the invariant features x_{in} through variational inference. Subsequently, a decoder network is introduced to estimate the clustering results, enabling post-intervention inference with

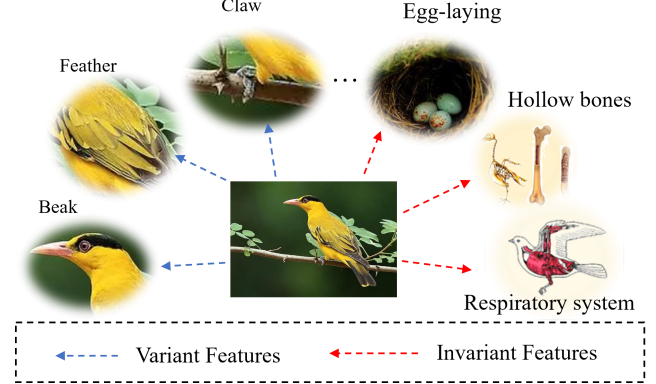


Figure 2. Illustration of the variant features and invariant features. Taking the bird for an example, the beak, feathers, and claws are considered variant features. In contrast, characteristics such as egg-laying, hollow bones, and other biosignatures are considered invariant features, which remain unchanged across different samples in the dataset.

partially aligned data features x'_{va} . Moreover, we incorporate a contrastive regularizer to explore correlations between samples, thereby enhancing the model’s discriminative capabilities. Comprehensive experiments on both fully and partially aligned datasets validate the efficacy and generalizability of our CauMVC model.

The primary contributions of our proposed CauMVC can be summarized as follows.

- We consider the model performance decreasing caused by data shift (i.e., from fully to partially aligned) as a generalized problem, formulating and solving it from causal perspective.
- We design a causal multi-view clustering network, employing causal modeling and inference to tackle the shift in multi-view input.
- Extensive experimentation on both fully and partially aligned data across eight benchmark datasets show the effectiveness and generalization of our method.

2. Preliminary

In this paper, we address the multi-view clustering task in scenarios with partial alignment. The raw features from different views represent various descriptions of the same sample. Therefore, in this setting, we consider the aligned data as the variant feature for the same sample cross different views. For a given dataset $\{x^{(v)}\}_{v=1}^V$, we randomly split the dataset into two partitions with 50% ratio, i.e., the aligned data and unaligned data. Let x_{va} and x_{in} denote the variant and invariant features, respectively. Here, we consider the unaligned data as the shift phenomenon compared with the aligned scenario, which is denoted as x'_{va} . The invariant features x_{in} are obtained by the encoder network $\mathcal{F}_\phi(\cdot)$.

¹ Video is collected from <https://www.youtube.com/watch?v=BwXWg3VipQE>.

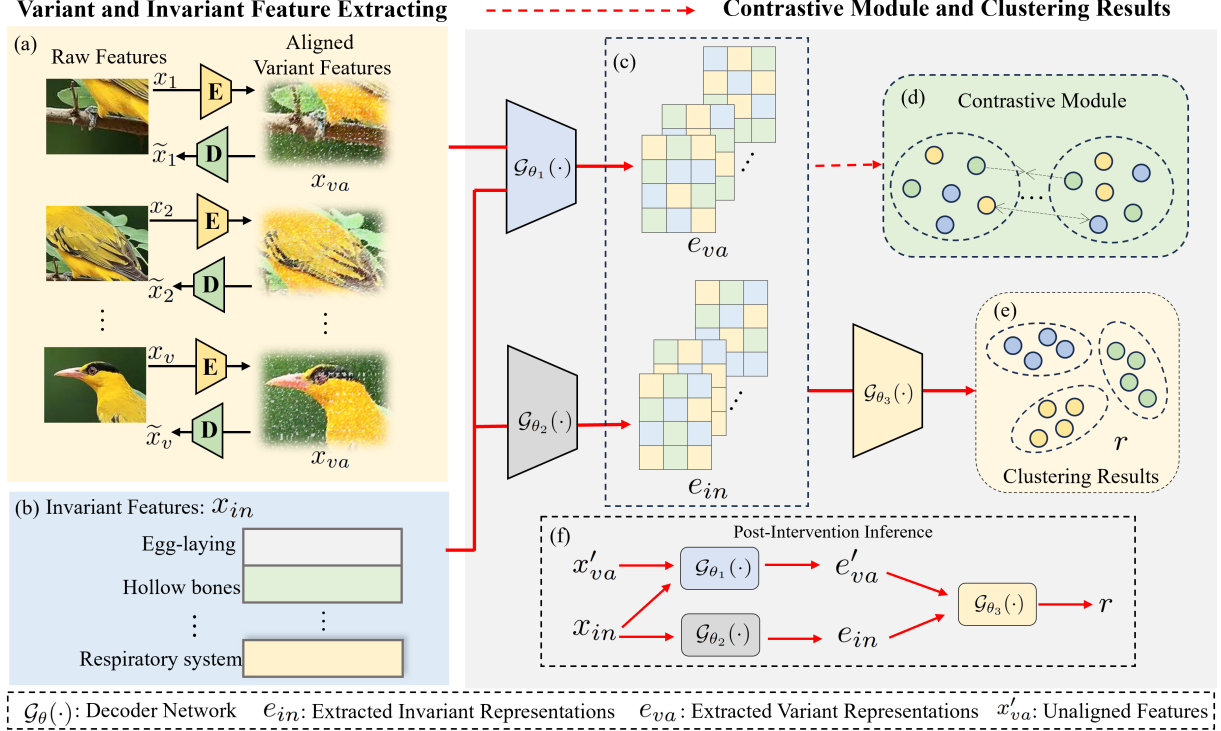


Figure 3. Illustration of the proposed causal multi-view clustering network. To be specific, we first design a autoencoder module (a) to obtain the variant features x_{va} and reconstruct the input raw features. Besides, the invariant features x_{in} are generated by the variational auto-encoder with the variant features and clustering results. Then, we construct the causal graph based on the variant features x_{va} and invariant features x_{in} . The variant and invariant representations are extracted by the network $\mathcal{G}_{\theta_1}(\cdot)$ and $\mathcal{G}_{\theta_2}(\cdot)$, respectively. Moreover, we design a contrastive module (d) to improve the discriminative capacity of the causal model. For the unaligned data, we utilize the causal graph to process the unaligned variant features x'_{va} and the invariant features x_{in} to generate the final clustering results r with performing the post-intervention inference.

Then, we obtain the extracted variant representations e_{va} and invariant representations e_{in} by the encoder networks \mathcal{G}_{θ_1} and \mathcal{G}_{θ_2} . Moreover, we define the clustering results as r . The fundamental notations used in this paper are outlined in Tab. 1.

3. Related Work

3.1. Multi-view Clustering

Recently, Multi-view Clustering (MVC) has garnered significant attention [13, 25, 32, 44, 60, 65, 75]. Existing MVC methods can be broadly categorized into two groups based on cross-view correspondence: MVC with fully aligned data and MVC with partially aligned data. Fully aligned data implies predefined mapping relationships for every pair of cross-view data. There are several works under this assumption, which can be encompassed in five main categories: (1) Non-negative matrix factorization-based MVC [50] aims to identify a shared latent factor, which is used to process information from multi-view input. (2) Kernel learning-based MVC [26, 27] involves predefining a base

kernels set for each views. After that, this method optimally fuse the weights of the kernels to improve clustering outcomes. (3) Subspace-based MVC [24] is based on the assumption that all views in the multi-view task share a low-dimensional latent space, with the final outcomes derived from learning this shared representation. (4) Benefiting from the successful of graph learning and its applications [28, 30, 31, 52, 59, 61–64, 66, 67], Graph-based MVC [20] seeks to constructing a unified graph from multiple views, with clustering results derived from spectral decomposition. (5) Thanks to the robust representational capabilities of deep networks [33, 34, 72–74], deep neural network-based MVC [4, 15, 16, 60] has the capacity to extract more sophisticated representations through neural networks. Despite achieving promising clustering performance, most of these methods heavily rely on the assumption that cross-view data are fully aligned.

To tackle this issue, many MVC algorithms have been proposed [14, 51, 56, 58]. PVC is designed to use a differentiable surrogate of the non-differentiable Hungarian algorithm to learn the correspondence of partially aligned

Notation	Meaning
x_{va}	Fully Aligned Variant Features
x_{in}	Invariant Features
x'_{va}	Partially Aligned Variant Features
e_{va}	Extracted Variant Representations
e_{in}	Extracted Invariant Representations
r	Clustering Results
$\mathcal{F}_\phi(\cdot)$	Variational Auto-Encoder Network
$\mathcal{G}_\theta(\cdot)$	Post-Intervention Inference Network
V	The Number of Views
N	The Number of Samples
Z	The Similarity Matrix

Table 1. Basic notations used in the whole paper.

data. MVC-UM [68], based on non-negative matrix factorization, learns the correspondence by exploring cross-view relationships. SURE [58] uses available pairs as positives and randomly selects some cross-view samples as negatives. UPMGC-SM [51] leverages structural information from each view to refine cross-view correspondences. In contrast to the above methods, we approach partially aligned data from a causal perspective, aiming to improve the generalization of the model.

3.2. Causal Disentangled Representation Learning

Traditional approaches for disentangled representation learning focus on examining mutually independent latent factors through the use of encoder-decoder networks. In this approach, a standard normal distribution is utilized as the prior for the latent code. Moreover, the variational posterior $q(z|x)$ is employed to approximate the unknown posterior $p(z|x)$. β -VAE [12] introduces an adaptive framework to adjust the weight of the KL term. Factor VAE [3] designs a framework, which focuses solely on the independence of factors. After that, the exploration of causal graphs from observations has gained significant attention, leveraging either purely observational data or a combination of observational and interventional data. NOTEARs [76] incorporates a novel Directed Acyclic Graph (DAG) constraint for causal learning. LiNGAM [38] ensures the identifiability of the model based on the assumptions of linear relationships and non-Gaussianity. In cases where interventions are feasible, Heckerman et al. [11] demonstrate the causal structure learned from interventional data can be identified. More recently, there has been an increasing interest in combining causality and disentangled representation. Suter et al. [40] employs causality to explain disentangled latent representations, while Kocaoglu et al. [19] introduces CausalGAN, a method supporting "do-operations" on images. Drawing inspiration from the success of causal learning, we apply causal modeling to multi-view clustering. To the best of our knowledge, our work represents the first attempt to lever-

age causal learning to improve model generalization with partially aligned data in the multi-view clustering task.

4. Method

In this section, we introduce a generalized multi-view clustering algorithm from a causal perspective. Specifically, we first present the relevant notations and formulations. Subsequently, We provide a detailed explanation of the causal multi-view clustering model and the contrastive regularizer. Finally, we introduce the training loss function of proposed CauMVC. The framework of CauMVC is shown in Fig. 3.

4.1. Problem Definition

4.1.1. Multi-view Clustering from Causal Perspective

In this paper, the objective is to achieve strong generalization in a partially aligned data environment via causal learning. We abstract the multi-view clustering process as a causal graph, shown in Fig.4. We provide the preliminary and symbol definitions in the Appendix. In following, we explain the rationality.

- x_{va}, x_{in} represent the variant features and invariant features, respectively. For instance, in the context of a bird dataset, the variant features include characteristics like the beak, feathers, and claws. invariant features can be considered as consistent features across different views, such as egg-laying animals, hollow bones, and respiratory system.
- e_{va} and e_{in} denote the extracted variant and invariant representations. e_{in} is isolated because there always exist representations that remain unaffected by x_{va} . For instance, the hollowness of bird bones is unrelated to the presence of feathers.
- r is the multi-view clustering results.
- $(x_{va}, x_{in}) \rightarrow e_{va}$ and $x_{in} \rightarrow e_{in}$ mean the extracted representations are determined by the input features.
- $(e_{va}, e_{in}) \rightarrow r$ is that the multi-view clustering task is affected by the extracted representations.

4.1.2. Multi-view Clustering with Partially Aligned Data

Multi-view clustering (MVC) seeks to uncover the shared clustering structure among various views, segmenting the multi-view data into distinct clusters in an unsupervised manner. In this work, we explore multi-view clustering task, where the input multi-view data is shift from aligned data x_{va} to partially aligned data x'_{va} . From the causal view, we termed the data shift as an intervention [35], which can be presented as $do(x_{va} = x'_{va})$. The primary objective is for the model to generalize and produce the post-intervention distribution of clustering.

4.2. Causal Multi-view Clustering Module

We consider the learning process illustrated in Fig.4 to construct the multi-view clustering model. To be specific, the

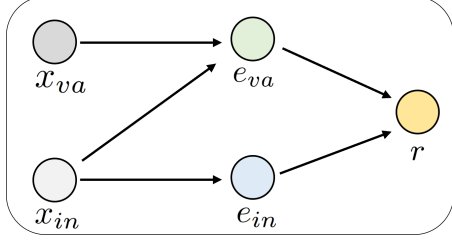


Figure 4. Causal graph illustrating the process of multi-view clustering. To be specific, x_{va} and x_{in} denote the variant features and invariant features, respectively. Then, the extracted variant and invariant representations e_{va} and e_{in} are obtained by the encoder network. Finally, the clustering results r are generated from e_{va} and e_{in} .

model commences by sampling a d-dimensional invariant features x_{in} from a standard Gaussian prior [21, 57]. From variant features x_{va} and invariant features x_{in} , we embed features to latent space and use e_{va} and e_{in} to produce multi-view clustering. Inspired by the prior works [21, 36, 57], we assume the features and the clustering results follow factorized Gaussian and multinomial priors, respectively. The distribution of x_{in}, e_{va}, e_{in} and r could be expressed as:

$$\begin{aligned} x_{in} &\sim \mathcal{N}(0, \mathbf{I}_d), \\ e_{va} &\sim \mathcal{N}(\mu_{\theta_1}(x_{va}, x_{in}), \text{diag}\{\sigma_{\theta_1}^2(x_{va}, x_{in})\}), \\ e_{in} &\sim \mathcal{N}(\mu_{\theta_2}(x_{in}), \text{diag}\{\sigma_{\theta_2}^2(x_{in})\}), \\ r &\sim \text{Mult}(\mathbf{R}, \pi(\mathcal{G}_{\theta_3}(e_{va}, e_{in}))), \end{aligned} \quad (1)$$

where $\theta_1(x_{va}, x_{in})$ represents the mean of the Gaussian distribution estimated from x_{va} and x_{in} by the function $\mathcal{G}_{\theta_1}(x_{va}, x_{in})$ parameterized by θ_1 . The term $\text{diag}\{\sigma_{\theta_1}^2(x_{va}, x_{in})\}$ represents the diagonal covariance of the Gaussian distribution. Similarly, $\mathcal{G}_{\theta_2}(x_{in})$ is employed to compute the mean and diagonal covariance of e_{in} . Moreover, the clustering results r is drawn from the multinomial distribution, which can be presented with parameters of $\mathbf{R} = \sum_{i=1}^N r_i$. Besides, $\pi(\mathcal{G}_{\theta_3}(e_{va}, e_{in}))$. $\pi(\cdot)$ is the softmax function used to normalize the output of $\mathcal{G}_{\theta_3}(e_{va}, e_{in})$.

To optimize the parameters $\theta_1, \theta_2, \theta_3$, we reconstruct r based on the variant features x_{va} . Concretely, for a multi-view data with x_{va} , we maximize the log-likelihood $\log p(r|x_{va})$, which can be expressed as:

$$\begin{aligned} \log p(r|x_{va}) &= \log \int p(r, x_{in}|x_{va}) dx_{in} \\ &= \log \int p(r|x_{va}, x_{in}) p(x_{in}) dx_{in}. \end{aligned} \quad (2)$$

However, due to the intractability of integrating over invariant features x_{in} in Eq. (2), we address this challenge

by drawing inspiration from variational inference [21, 49]. Specifically, we introduce a variational distribution $q(x_{in}|\cdot)$ to derive the evidence lower bound (ELBO) of Eq. (2) as:

$$\begin{aligned} \log p(r|x_{va}) &= \log \int p(r|x_{va}, x_{in}) p(x_{in}) \frac{q(x_{in}|\cdot)}{q(x_{in}|\cdot)} dx_{in} \\ &\geq \mathbb{E}_{q(x_{in}|\cdot)} \left[\log \frac{p(r|x_{va}, x_{in}) p(x_{in})}{q(x_{in}|\cdot)} \right] \\ &= \mathbb{E}_{q(x_{in}|\cdot)} [\log p(r|x_{va}, x_{in})] \\ &\quad - \text{KL}(q(x_{in}|\cdot) || p(x_{in})), \end{aligned} \quad (3)$$

where the first term in Eq.(3) aims to reconstruct while the second term is to regularize the Kullback-Leibler divergence between $q(x_{in}|\cdot)$ and the prior $p(x_{in})$. The goal is to maximize the ELBO in Eq.(3), thereby increasing the log-likelihood in Eq.(2). To achieve this objective, we design the variational auto-encoder and decoder network to model $q(x_{in}|\cdot)$ and $p(r|x_{va}, x_{in})$, respectively.

4.2.1. Variational Auto-Encoder

Invariant features reflect the fundamental attributes of the data, which remain consistent regardless of changes in perspective. **However, how to obtain the invariant features is a challenging problem.** In this work, we attempt to infer the invariant features from the existing information. To be specific, we assume that the clustering results and the variant features are likely to indicate the invariant features. Taking the bird dataset for example, animals characterized by features such as feathers and beaks, and subsequently classified as birds through clustering algorithms, are likely to exhibit biological traits such as egg-laying and possessing hollow bones. Therefore, we define $q(x_{in}|\cdot) = q(x_{in}|r', x_{va})$. To efficiently estimate of $q(x_{in}|r', x_{va})$, we employ amortized inference [10] and integrate an encoder network. This process can be described as follows:

$$q(x_{in}|r', x_{va}) = \mathcal{N}(x_{in}; \mu_{\varphi}(r', x_{va}), \text{diag}\{\sigma_{\varphi}^2(r', x_{va})\}), \quad (4)$$

where $\mu_{\varphi}(\cdot)$ and $\sigma_{\varphi}(\cdot)$ are the parameters obtained by the encoder network $\mathcal{F}_{\varphi}(\cdot)$, i.e., $\mathcal{F}_{\varphi}(r, x_{va}) = [\mu_{\varphi}(r, x_{va}), \sigma_{\varphi}(r, x_{va})]$. r' is the clustering results obtained by the pretrain model. We employ the multi-layer perception (MLP) as encoder network $\mathcal{F}_{\varphi}(\cdot)$.

4.2.2. Decoder Network

We decompose $p(r|x_{va}, x_{in})$ according to Eq.(1), which can be expressed as:

$$p(r|x_{va}, x_{in}) = \int \int p(e_{va}|x_{va}, x_{in}) p(e_{in}|x_{in}) p(r|e_{va}, e_{in}) de_{va} de_{in}, \quad (5)$$

where the parameters of $p(e_{va}|x_{va}, x_{in})$ and $p(e_{in}|x_{in})$ are determined by $\mathcal{G}_{\theta_1}(x_{va}, x_{in})$ and $\mathcal{G}_{\theta_2}(x_{in})$, re-

spectively. Similar to encoder network, we employ decoder networks by two MLPs, denoted as $\mathcal{G}_{\theta_1}(x_{va}, x_{in}) = [\mu_{\theta_1}(x_{va}, x_{in}), \sigma_{\theta_1}(x_{va}, x_{in})]$ and $\mathcal{G}_{\theta_2} = [\mu_{\theta_2}(x_{in})], \sigma_{\theta_2}(x_{in})$.

4.2.3. Approximation Process

Though the above analysis, we could obtain the estimations of $p(e_{va}|x_{va}, x_{in})$ and $p(e_{in}|x_{in})$. However, the calculation of $p(r|x_{va}, x_{in})$ is challenging due to the computationally expensive integration over the variables e_{va} and e_{in} . Consequently, we utilize Monte Carlo sampling [37] to enhance efficiency. Formally,

$$p(r|x_{va}, x_{in}) \approx \frac{1}{A} \frac{1}{B} \sum_{a=1}^A \sum_{b=1}^B p(r|e_{va}^a, e_{in}^b), \quad (6)$$

where A and B are the sample numbers. Besides, e_{va}^a and e_{in}^b are drawn from the distributions $p(e_{va}|x_{va}, x_{in})$ and $p(e_{in}|x_{in})$, respectively. However, the computationally cost associated with Eq.(7) remains high due to the necessity of calculating the conditional probability for $A \times B$ iterations. To address this challenge, we employ a widely adopted approximation technique [7, 48] as:

$$p(r|x_{va}, x_{in}) \approx p\left(r \mid \frac{1}{A} \sum_{a=1}^A e_{va}^a, \frac{1}{B} \sum_{b=1}^B e_{in}^b\right) = p(r|\bar{e}_{va}, \bar{e}_{in}), \quad (7)$$

where the approximation error (Jensen gap [1]) can be effectively bounded for most functions when calculating $p(r|\bar{e}_{va}, \bar{e}_{in})$ [48]. We employ an MLP as the backbone for $\mathcal{G}_{\theta_3}(\cdot)$. Therefore, we can estimate the parameters of $p(r|\bar{e}_{va}, \bar{e}_{in})$. The reconstruction term $\log p(r|x_{va}, x_{in})$ can be calculated as follows:

$$\log p(r|\bar{e}_{va}, \bar{e}_{in}) \stackrel{c}{=} \sum_{i=1}^N r'_i \log \pi(\mathcal{G}_{\theta_3}(\bar{e}_{va}, \bar{e}_{in})), \quad (8)$$

where r'_i represents the clustering results of the multi-view data obtained by the pretrain model. $\pi(\mathcal{G}_{\theta_3}(\cdot))$ signifies the prediction of the i -th sample after applying softmax normalization $\pi(\cdot)$ to the output of $\mathcal{G}_{\theta_3}(\cdot)$. Specifically, Eq.(8) determines the reconstruction probability of obtaining r from the multinomial distribution by performing R times.

In summary, our goal is to maximize the Evidence Lower Bound (ELBO) in Eq.(3) in order to optimize φ and $\theta = \{\theta_1, \theta_2, \theta_3\}$. Moreover, following [21, 49], we utilize the KL annealing to regulate the KL divergence regularization. The ELBO loss function can be presented as:

$$\mathcal{L}_{ELBO} = \mathbb{E}_{q_{\varphi}(x_{in}|r, x_{va})} [\log p_{\theta}(r|x_{va}, x_{in})] - \text{KL}(q_{\varphi}(x_{in}|r, x_{va}) || p(x_{in})). \quad (9)$$

4.2.4. Causal Inference of Multi-view Clustering with Partially Aligned Data

After that, we provide the explanation of how to infer the post-intervention probabilities $p(r|x'_{va}, x_{in})$, where x'_{va} denotes the shift data, i.e., partially aligned multi-view data.

Concretely, the causal inference is divided into two steps. Firstly, we acquire the invariant features based on Eq.(4), which can be formulated as:

$$q(x_{in}|r, x'_{va}) = \mathcal{N}(x_{in}; \mu_{\varphi}(r, x'_{va}), \text{diag}\{\sigma_{\varphi}^2(r, x'_{va})\}). \quad (10)$$

Then, according to Eq.(5), we feed x'_{va} and x_{in} to the decoder model to generate the post-intervention probabilities as:

$$p(r|x'_{va}, x_{in}) = \int \int p(e'_{va}|x'_{va}, x_{in}) p(e_{in}|x_{in}) p(r|e'_{va}, e_{in}) de'_{va} de_{in}, \quad (11)$$

4.3. Contrastive Regularizer

In this subsection, we design a contrastive regularizer to mine the relationship between samples. Specifically, we compute the similarity matrix \mathbf{Z} between the variant representations e_{va} and invariant representations e_{in} :

$$\mathbf{Z} = \frac{(e_{va}) (e_{in})^T}{\|e_{va}\|_2 \|e_{in}\|_2}. \quad (12)$$

Then, we constrain the \mathbf{Z} to be close to an identity matrix \mathbf{I} . The contrastive loss can be presented as:

$$\begin{aligned} \mathcal{L}_C &= \frac{1}{N^2} \sum (\mathbf{Z} - \mathbf{I})^2 \\ &= \frac{1}{N} \sum_{i=1}^N (\mathbf{Z}_{ii} - 1)^2 + \frac{1}{N^2 - N} \sum_{i=1}^N \sum_{j \neq i} (\mathbf{Z}_{ij})^2, \end{aligned} \quad (13)$$

where the initial term in Eq.(13) compels the diagonal elements of \mathbf{Z} to 1. This operation encourages the representations of the same sample to agree with each other in latent space. Moreover, the latter term drives the off-diagonal elements to approach 0, thus pushing apart the representations of different samples.

4.4. Loss Function

Autoencoder[5, 60] is widely used in multi-view clustering. In this work, we utilize an autoencoder to learn the semantics across different views in the latent space. The reconstructed loss is calculated as:

$$\mathcal{L}_R = \sum_{v=1}^V \|x_{va}^v - \tilde{x}_o^v\|_F^2, \quad (14)$$

where x_{va} and \tilde{x}_o denote input observed multi-view feature and reconstructed features, respectively. The loss function of our proposed CauMVC mainly include three components, i.e., the reconstructed loss \mathcal{L}_R , the ELBO loss

Algorithm 1 Inference Pipeline of CauMVC with Partially Aligned Data

Input: The partially aligned data x'_{va} ; the iteration number I
Output: The clustering result r .

```
1: for  $i = 1$  to  $I$  do
2:   Obtain the invariant features  $x_{in}$  by  $\mathcal{F}_{\varphi}(\cdot)$  with Eq. (10).
3:   Encoder the representations  $e'_{va}$  and  $e_{in}$  by  $\mathcal{G}_{\theta_1}$  and  $\mathcal{G}_{\theta_2}$ .
4:   Obtain the post-intervention inference  $r$  with Eq. (11).
5:   Calculate the ELBO loss, contrastive loss, and
     reconstruction loss with Eq. (9), (13) and (14).
6:   Calculate the total loss  $\mathcal{L}$  by Eq. (15).
7:   Update model by minimizing  $\mathcal{L}$  with Adam optimizer.
8: end for
9: return  $r$ 
```

\mathcal{L}_{ELBO} and the contrastive loss \mathcal{L}_C . Overall, the loss function can be calculated as:

$$\mathcal{L} = \mathcal{L}_R + \alpha \mathcal{L}_{ELBO} + \beta \mathcal{L}_C, \quad (15)$$

where α and β are the trade-off hyper-parameters. Detailed training procedure is presented in Alg. 1.

5. Experiments

In this section, we implement experiments to validate the superiority of CauMVC by addressing the following raised questions (**RQ**): **RQ1**: How does CauMVC compare with other leading deep multi-view clustering techniques in terms of performance? **RQ2**: In what ways do the essential components of CauMVC enhance multi-view clustering results? **RQ3**: What is the effect of hyper-parameters on the efficacy of CauMVC? **RQ4**: What clustering structures are identified by CauMVC?

5.1. Datasets & Metric

To assess the effectiveness of our proposed CauMVC, we conduct comprehensive experiments on eight widely used datasets, including BBCSport, Reuters, Caltech101-7, UCI-digit, Movies, WebKB, SUNRGB-D, and STL-10. A summary of the key information regarding these datasets is presented in Tab. 3. Besides, we adopt the commonly used metrics to verify the model performance, including clustering accuracy (ACC) [61, 64], normalized mutual information (NMI) [29, 62], and purity (PUR) [54].

5.2. Experiment Setup

Our experiments are conducted on the PyTorch platform utilizing an NVIDIA 3090 GPU. For all baseline methods, we replicate the results using the original source code and configurations provided by the authors. DealMVC [60] is employed as the pretraining model to obtain the clustering results. In the proposed method, the algorithm is optimized using the Adam optimizer [18]. The learning rate is set to

3e-3 for the BBCSport, Caltech-7, UCI-digit, and STL-10 datasets, and 5e-3 for the Movies dataset. The training is conducted for 500 epochs with a batch size of 256 for all datasets. The trade-off hyper-parameters α and β are consistently set to 1.0. Detailed hyper-parameter settings are presented in Tab. 4.

To show the effectiveness and generalization of our CauMVC, we implement performance comparison experiments for our proposed CauMVC and 14 baselines, which can be divided into two groups, i.e., nine compared multi-view clustering algorithms with fully aligned data (SDMVC [53], CoMVC [42], SiMVC [42], SD-SNE [22], MFLVC [54], DSMVC [41], GCFAggMVC [55], DealMVC [60], TGM-MVC [47]), five compared methods with partially aligned data (PVC [14], MvCLN [56], SURE [58], MVC-UM [68], RMCNC [39]).

5.3. Performance Comparison (RQ1)

To evaluate the generalization capability of CauMVC, we conducted experiments on both aligned and partially aligned datasets, comparing the results against 11 baseline methods. Firstly, we construct the partially aligned data based on the eight datasets. To be concrete, following PVC [14], we randomly split the data into two partitions $\{\mathbf{x}_{va}^{(v)}, \mathbf{x}_{va}^{'(v)}\}_{v=1}^V$ with 50% ratio.

The comparative experimental results are shown in Tab. 2 and Tab. 5. We highlight the optimal results in bold, and the sub-optimal results with an underline. From those results, we have the following observations: (1) In the fully aligned data scenario, our CauMVC outperforms other multi-view clustering methods on eight datasets. Taking the results on the Caltech101-7 dataset as an example, CauMVC surpasses the second-best multi-view clustering method by 1.72%, 2.30%, and 1.72% in ACC, NMI, and PUR, respectively. (2) CauMVC demonstrates promising clustering performance when dealing with partially aligned data. We attribute this to CauMVC's use of causal modeling in the multi-view clustering process and its ability to estimate the post-intervention probability. (3) CauMVC achieves superior performance in both fully aligned data and partially aligned data scenarios. The high performance showcases the strong generalization ability of CauMVC under data shifts, from fully aligned data to partially aligned data. In summary, the above observations confirm the remarkable performance of our proposed CauMVC.

Influence of Different Aligned Ratios: Moreover, we perform additional experiments to investigate the model performance across various aligned ratios on eight datasets. The aligned ratio ranges from 0.5 to 0.9. The results for ACC, NMI, and PUR are illustrated in Fig. 12. It is evident that CauMVC surpasses other baseline models across different aligned ratios in most scenarios. This indicates the robust generalization capability of CauMVC in managing

Aligned	Mthods		Movies			UCI-digit			STL10			SUNRGBD		
	Evaluation metrics		ACC	NMI	PUR									
Fully	SDMVC	TKDE 2021	27.71	26.07	30.28	63.00	64.29	67.05	30.01	25.27	31.07	17.22	14.11	21.53
	CoMVC	CVPR2021	17.50	14.45	19.45	46.40	49.36	46.45	23.55	16.26	25.01	16.03	11.59	21.60
	SiMVC	CVPR2021	17.18	14.64	18.80	20.75	16.59	21.75	16.04	06.34	17.02	13.44	10.52	21.63
	SDSNE	AAAI 2022	<u>29.34</u>	<u>26.32</u>	<u>30.31</u>	84.55	89.05	<u>87.05</u>	O/M	O/M	O/M	O/M	O/M	O/M
	MFLVC	CVPR 2022	20.75	22.05	23.99	87.00	80.40	87.00	31.14	25.36	31.25	13.22	13.69	23.12
	DSMVC	CVPR 2022	17.02	12.60	19.12	85.45	80.67	85.40	27.53	19.33	29.41	17.76	10.43	10.50
	GCFAggMVC	CVPR 2023	26.42	25.43	26.98	81.55	77.70	81.55	<u>36.69</u>	28.78	<u>38.36</u>	17.98	<u>13.86</u>	22.64
	DealMVC	ACM MM 2023	26.42	23.79	28.20	86.20	81.78	86.20	36.44	29.93	36.95	<u>18.16</u>	08.58	19.17
	TGM-MVC	ACM MM 2024	17.18	16.80	18.96	54.35	62.76	59.40	26.18	<u>30.86</u>	27.51	15.37	13.80	<u>23.20</u>
	CauMVC	Ours	29.98	26.41	30.96	91.85	85.90	91.85	37.88	31.30	38.95	18.83	14.68	24.20
Partially	PVC	NeurIPS 2020	14.26	13.29	<u>16.53</u>	<u>77.30</u>	75.54	80.50	26.18	25.22	<u>31.33</u>	10.71	11.28	<u>19.33</u>
	MvGLN	CVPR 2021	14.39	10.87	15.79	66.78	58.93	67.48	10.00	09.06	10.00	09.97	09.79	11.40
	MVC-UM	KDD 2021	<u>23.76</u>	<u>26.42</u>	13.50	61.09	56.61	63.60	O/M	O/M	O/M	10.34	12.93	18.73
	SURE	TPAMI 2023	14.82	11.92	16.24	51.76	37.64	52.56	23.82	13.20	25.00	11.11	13.11	16.43
	RCMCN	TKDE 2024	14.10	09.87	13.24	50.64	36.87	51.97	21.65	14.54	23.75	<u>14.65</u>	<u>14.12</u>	19.24
	CauMVC	Ours	25.78	26.84	26.56	80.99	77.06	81.12	33.89	27.95	34.73	15.39	15.12	23.61

Table 2. Multi-view clustering performance on eight benchmark datasets (Part 1/2). The optimal results are marked in **bold**, and the sub-optimal values are underlined.

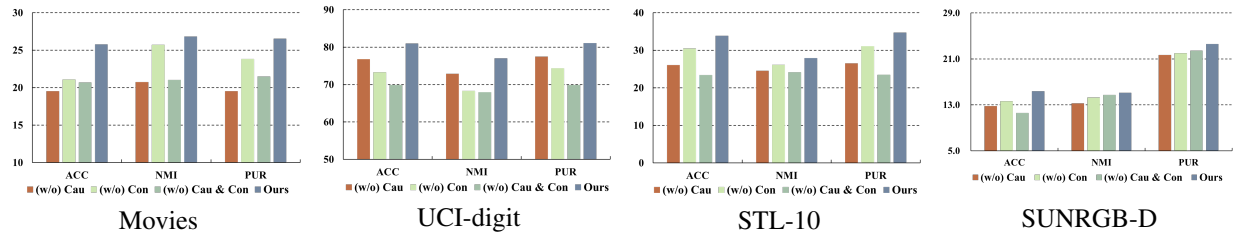


Figure 5. Ablation studies on four datasets with partially aligned data. “(w/o) Cau”, “(w/o) Con”, “(w/o) Cau&Con”, and “Ours” correspond to reduced models by individually removing the causal module, the contrastive regularizer, and all aforementioned modules combined, respectively.

Dataset	Samples	Clusters	Views
BBCSport	544	5	2
Movies	617	17	2
WebKB	1051	2	2
Reuters	1200	6	5
Caltech101-7	1400	7	5
UCI-digit	2000	10	3
SUNRGB-D	10335	45	3
STL-10	13000	10	4

Table 3. Dataset summary in this paper.

partially aligned data.

5.4. Ablation Studies (RQ2)

In this subsection, we conduct ablation studies with partially aligned data to verify the effectiveness of our designed modules, i.e. causal module and contrastive regularizer. Concretely, “(w/o) Cau”, “(w/o) Con”, “(w/o) Cau&Con”, and “Ours” represent the ablated models where the causal module, the contrastive regularizer, and both modules combined, respectively, are individually removed. In the “(w/o) Cau&Con” configuration, we employ an autoencoder net-

work as the backbone to derive representations for the downstream clustering task. The corresponding results are illustrated in Fig. 10. The findings indicate that omitting any of the proposed modules results in a significant reduction in clustering performance, highlighting the critical contribution of each designed module to the overall efficacy. We further delve into the underlying reasons as follows: (1) We resort the multi-view clustering from the causal perspective. The model generalization is improved when the input is partially aligned data, thus achieving promising performance. (2) The contrastive module could push the positive sample close, and pull the negative sample away, enhancing the model’s discriminative capacity. The model could achieve better clustering outcomes. Besides, we perform ablation studies with fully aligned data to assess the effectiveness of our designed modules, namely the causal module and contrastive regularizer. The results in Fig. 2 of the Appendix clearly demonstrate that eliminating any of the designed modules results in a significant drop in clustering performance. This underscores the crucial role each module plays in achieving optimal overall performance.

	Dataset	BBCSport	Movies	WebKB	Reuters	Caltech101-7	UCI-digit	SUNRGB-D	STL-10
Statistics	Samples	544	617	1051	1200	1400	2000	10335	13000
	Clusters	5	17	2	6	7	10	45	10
	Views	2	2	2	5	5	3	3	4
Hyper-parameters	α	1.0	1.0	1.0	1.0	1.0	1.0	1.0	1.0
	β	1.0	1.0	1.0	1.0	1.0	1.0	1.0	1.0
	Learning Rate	0.003	0.005	0.003	0.003	0.003	0.003	0.003	0.003

Table 4. Statistics and hyper-parameter settings of eight benchmark datasets.

Aligned	Mthods			BBCSport			Reuters			Caltech101-7			WebKB		
	Evaluation metrics			ACC	NMI	PUR	ACC	NMI	PUR	ACC	NMI	PUR	ACC	NMI	PUR
Fully	SDMVC	TKDE 2021	51.29	32.86	57.23	17.67	14.73	18.58	44.21	30.97	47.93	75.07	16.30	78.12	
	CoMVC	CVPR 2021	37.50	09.82	40.81	32.25	13.58	33.83	40.84	28.66	69.95	66.03	13.66	78.12	
	SiMVC	CVPR 2021	37.87	10.99	40.07	33.58	10.36	33.67	75.03	37.07	77.54	72.79	10.31	78.12	
	SDSNE	AAAI 2022	76.62	57.50	75.84	23.25	20.28	27.00	76.14	74.52	78.93	76.19	14.55	76.19	
	MFLVC	CVPR 2022	40.99	27.79	61.46	39.92	20.01	41.42	80.40	70.30	80.40	71.65	15.95	78.12	
	DSMVC	CVPR 2022	41.91	14.67	47.59	43.83	18.11	45.00	62.64	47.34	64.43	64.41	11.62	78.12	
	GCFAggMVC	CVPR 2023	59.01	39.27	66.91	38.83	21.47	39.92	83.36	73.31	83.66	74.65	15.47	78.99	
	DealMVC	ACM MM 2023	<u>80.70</u>	65.59	<u>80.70</u>	<u>47.05</u>	26.32	48.36	<u>88.71</u>	<u>80.95</u>	<u>88.71</u>	79.26	15.32	79.26	
	TGM-MVC	ACM MM 2024	39.15	17.92	39.89	42.42	<u>29.65</u>	42.91	86.44	78.67	83.64	<u>79.64</u>	<u>16.61</u>	<u>79.64</u>	
	CauMVC	Ours	83.09	<u>64.31</u>	83.09	49.08	30.43	52.08	90.43	83.25	90.43	81.44	22.37	81.44	
Partially	PVC	NeurIPS 2020	35.66	00.36	35.66	16.83	00.04	16.83	46.00	29.15	44.83	54.12	12.47	68.12	
	MvGLN	CVPR 2021	32.39	04.80	<u>44.82</u>	<u>32.84</u>	11.82	<u>35.32</u>	<u>48.97</u>	35.77	45.12	54.70	<u>12.74</u>	73.70	
	MVC-UM	KDD 2021	<u>35.85</u>	<u>14.75</u>	36.21	17.00	00.82	17.08	41.52	<u>47.52</u>	83.39	52.15	11.34	70.21	
	SURE	TPAMI 2023	30.96	01.94	36.03	26.53	04.91	27.80	32.31	22.57	34.20	<u>55.85</u>	10.15	<u>74.12</u>	
	RMCNC	TKDE 2024	27.57	11.13	27.65	21.45	<u>18.54</u>	23.49	42.87	34.51	43.46	50.24	11.58	73.09	
	CauMVC	Ours	56.64	36.87	56.64	43.36	21.23	46.09	70.90	54.54	<u>70.90</u>	57.62	14.37	75.98	

Table 5. Multi-view clustering performance on eight benchmark datasets (Part 2/2). The optimal results are marked in **bold**, and the sub-optimal values are underlined.

5.5. Hyper-parameter Analysis (RQ3)

To further examine the impact of the parameters α and β on our model, we conducted experiments using UCI-digit dataset. In particular, we analyzed parameter values within the range of $\{0.01, 0.1, 1.0, 10, 100\}$. According to the results presented in Fig. 9. We could find the following observations. (1) When α and β are assigned extreme values (0.1 or 100), the clustering performance tends to decline. We speculate that this decline is due to the disruption of the loss function balance. Additionally, the model demonstrates optimal performance when the trade-off parameters are approximately 1.0. (2) From the results, we find that α has a more pronounced effect on model performance, suggesting that the causal model greatly enhances the overall efficacy of the model.

5.6. Visualization Experiment (RQ4)

In this subsection, we utilize visualization method to intuitively demonstrate the effectiveness of CauMVC. Specifically, we use the t-SNE [43] algorithm as the baseline to visualize the distribution of the learned embeddings of CauMVC on the UCI-digit dataset. The experimental results are presented in Fig.15, the results indicate that, with the training procedure, CauMVC more effectively reveals the intrinsic clustering structure compared to the raw fea-

tures. More detailed visualizations of the experiments are presented in Fig.6 in the Appendix.

6. Conclusion

In this paper, we consider the model performance decreasing caused by data shift as a generalization problem. The objective of model is to achieve strong generalization on both fully and partially aligned data. We formulate this issue from a causal view, and design CauMVC to perform causal modeling of the procedure. Then, we conduct post-intervention inference to obtain the clustering results. Moreover, we design a contrastive regularizer to improve the discriminative capacity of the model. Extensive experiments on both fully aligned and partially aligned data have demonstrated the strong generalization and effectiveness of our CauMVC. This paper makes an initial attempt to explore model generalization through causal representation learning. In the future, how to deal with more challenging problem into a uniform causal framework is a interesting direction, such as incomplete data and noisy data.

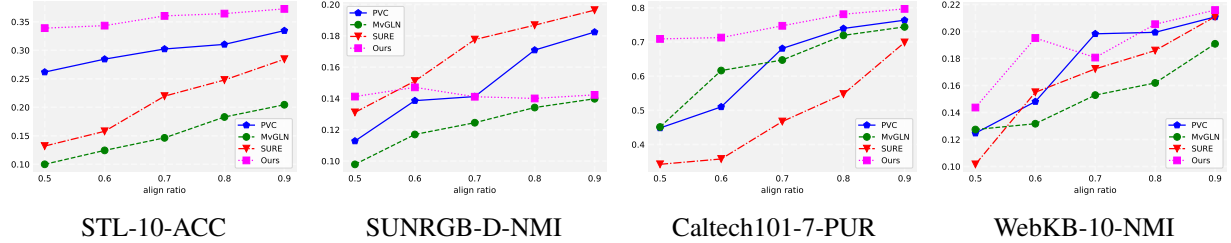


Figure 6. Clustering performance on four Datasets with different aligned ratios.

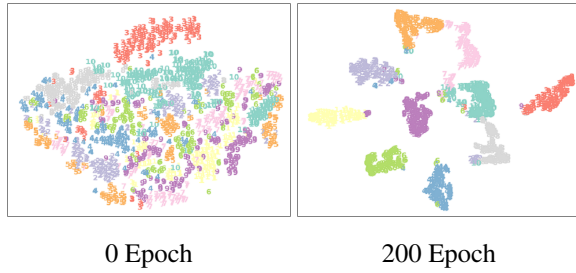


Figure 7. Visualization of the representations during the training process on UCI-digit dataset.

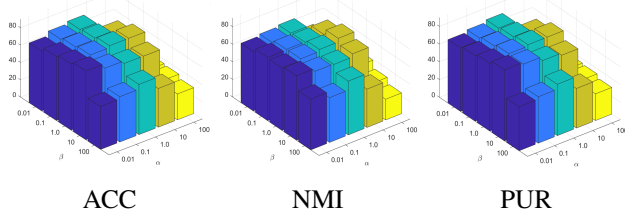


Figure 8. Sensitivity analysis of the hyper-parameter α and β on UCI-digit datasets.

7. Acknowledgments

This work is supported in by the National Science and Technology Innovation 2030 Major Project of China under Grant No. 2022ZD0209103, the Major Program Project of Xiangjiang Laboratory under Grant No. 24XJJCYJ01002, the National Science Fund for Distinguished Young Scholars of China under Grant No. 62325604, the National Natural Science Foundation of China (project No. 62406329, 62476280, 62276271, 62476281, 62406329), the National Natural Science Foundation of China Joint Found under Grant No. U24A20323, and the Program of China Scholarship Council (No. 202406110009).

A. Additional Experiments

A.1. Ablation Studies

In this section, we first present the ablation study on all datasets under the partially aligned scenario. “(w/o) Cau”, “(w/o) Con”, “(w/o) Cau&Con”, and “Ours” represent the ablated models where the causal module, the contrastive

regularizer, and both modules combined, respectively, are individually removed. In the “(w/o) Cau&Con” configuration, we employ an autoencoder network as the backbone to derive representations for the downstream clustering task. Consistent with the conclusions drawn in the main text, the results are summarized as follows.

- We resort the multi-view clustering from the causal perspective. The model generalization is improved when the input is partially aligned data, thus achieving promising performance.
- The contrastive module could push the positive sample close, and pull the negative sample away, enhancing the model’s discriminative capacity. The model could achieve better clustering outcomes.

Besides, we perform ablation studies with fully aligned data to assess the effectiveness of our designed modules, namely the causal module and contrastive regularizer. Specifically, “(w/o) Cau,” “(w/o) Con,” “(w/o) Cau&Con,” and “Ours” denote reduced models created by individually omitting the causal module, the contrastive regularizer, and both modules together. In this paper, we employ an autoencoder network as the core architecture to derive representations for the subsequent clustering task, referred to as “(w/o) Cau&Con.”. The outcomes are depicted in Fig. 11. These results clearly demonstrate that the exclusion of any of the designed modules leads to a significant decrease in clustering performance, underscoring the essential role each module plays in optimizing overall performance.

A.2. Different Align Ratio

To evaluate the performance of CauMVC under different alignment ratios, we conduct experiments on eight datasets, with the results presented in Fig. 12, Fig. 13, and Fig. 14. The results clearly demonstrate that CauMVC outperforms other baseline models across various alignment ratios in most scenarios. This highlights its strong generalization capability in handling partially aligned data effectively.

A.3. Sensitivity Analysis of α and β

To further investigate the impact of the parameters α and β on our model, we conduct experiments on the BBC-Sport dataset, analyzing parameter values within the range

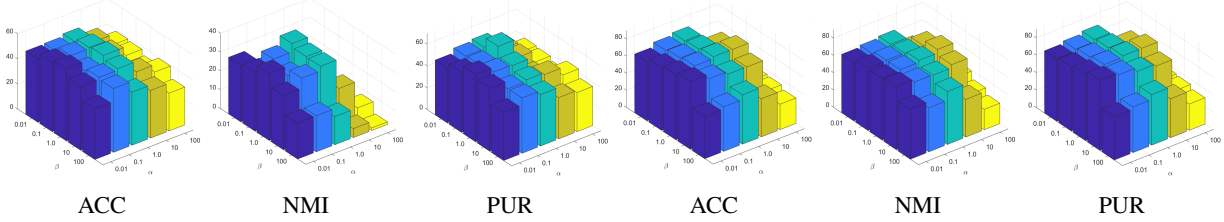


Figure 9. Sensitivity analysis of the hyper-parameter α and β on BBCSport and UCI-digit datasets.

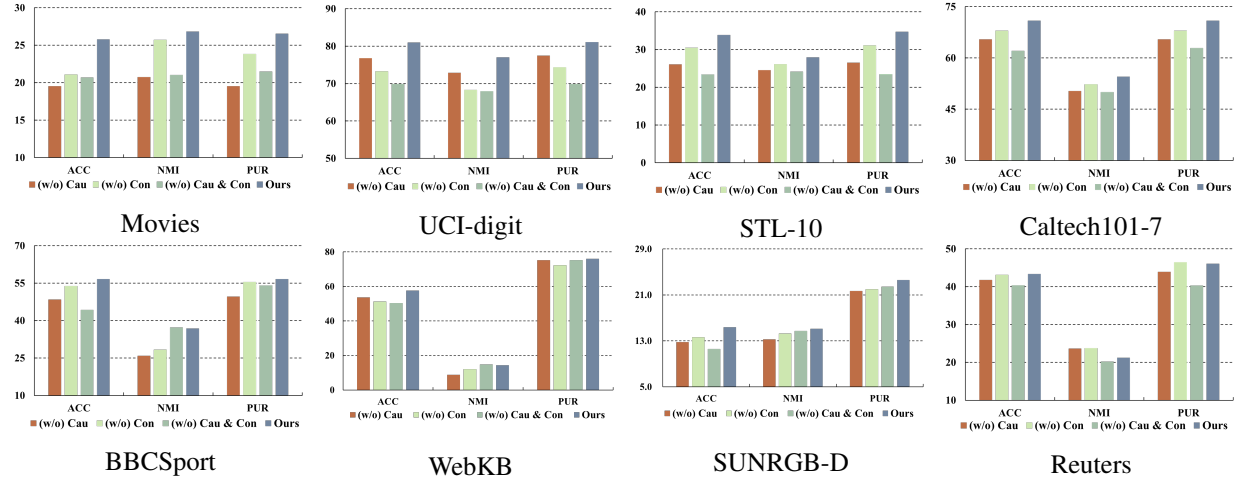


Figure 10. Ablation studies on eight datasets with partially aligned data. “(w/o) Cau”, “(w/o) Con”, “(w/o) Cau&Con”, and “Ours” correspond to reduced models by individually removing the causal module, the contrastive regularizer, and all aforementioned modules combined, respectively.

of $\{0.01, 0.1, 1.0, 10, 100\}$. Due to space constraints, the experimental results for the BBCSport dataset are provided in the Appendix. Based on the results presented in Fig. 9, we draw the following observations:

- When α and β are assigned extreme values (0.1 or 100), the clustering performance tends to degrade. We hypothesize that this decline results from an imbalance in the loss function. Moreover, the model achieves optimal performance when the trade-off parameters are set around 1.0.
- The results also indicate that α has a more significant impact on model performance, suggesting that the causal model plays a crucial role in enhancing the overall effectiveness of the approach.

References

- [1] Shoshana Abramovich and Lars-Erik Persson. Some new estimates of the ‘jensen gap’. *Journal of Inequalities and Applications*, 2016(1):1–9, 2016. 6
- [2] Huayue Cai, Xiang Zhang, Long Lan, Guohua Dong, Chuanfu Xu, Xinwang Liu, and Zhigang Luo. Learning deep discriminative embeddings via joint rescaled features and log-probability centers. *Pattern Recognition*, 114:107852, 2021. 1
- [3] Ricky TQ Chen, Xuechen Li, Roger B Grosse, and David K Duvenaud. Isolating sources of disentanglement in variational autoencoders. *Advances in neural information processing systems*, 31, 2018. 4
- [4] Yuzhuo Dai, Jiaqi Jin, Zhibin Dong, Siwei Wang, Xinwang Liu, En Zhu, Xihong Yang, Xinbiao Gan, and Yu Feng. Imputation-free and alignment-free: Incomplete multi-view clustering driven by consensus semantic learning. In *Proceedings of the Computer Vision and Pattern Recognition Conference*, pages 5071–5081, 2025. 3
- [5] Zhibin Dong, Siwei Wang, Jiaqi Jin, Xinwang Liu, and En Zhu. Cross-view topology based consistent and complementary information for deep multi-view clustering. In *Proceedings of the IEEE/CVF International Conference on Computer Vision*, pages 19440–19451, 2023. 6
- [6] Zhibin Dong, Meng Liu, Siwei Wang, Ke Liang, Yi Zhang, Suyuan Liu, Jiaqi Jin, Xinwang Liu, and En Zhu. Enhanced then progressive fusion with view graph for multi-view clustering. In *Proceedings of the Computer Vision and Pattern Recognition Conference*, pages 15518–15527, 2025. 1
- [7] Xiang Gao, Meera Sitharam, and Adrian E Roitberg. Bounds on the jensen gap, and implications for mean-concentrated distributions. *arXiv preprint arXiv:1712.05267*, 2017. 6
- [8] Zhirui Gao, Renjiao Yi, Zheng Qin, Yunfan Ye, Chenyang Zhu, and Kai Xu. Learning accurate template match-

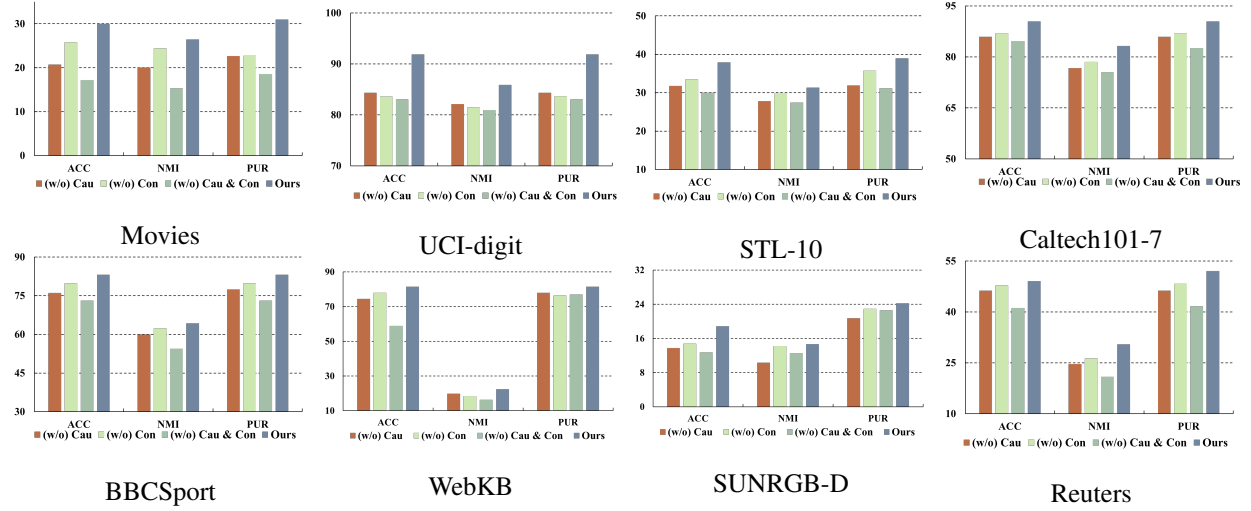


Figure 11. Ablation studies on eight datasets with fully aligned data. “(w/o) Cau”, “(w/o) Con”, “(w/o) Cau&Con”, and “Ours” correspond to reduced models by individually removing the causal module, the contrastive regularizer, and all aforementioned modules combined, respectively.

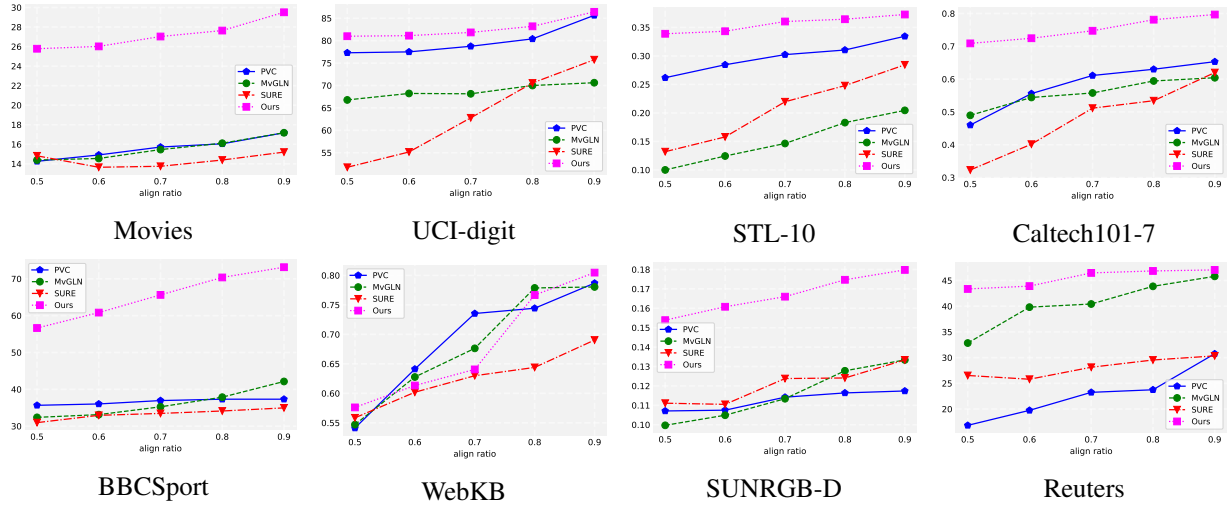


Figure 12. Clustering performance on eight Datasets with different aligned ratios in accuracy metrics.

ing with differentiable coarse-to-fine correspondence refinement. *Computational Visual Media*, 10(2):309–330, 2024. 1

[9] Zhirui Gao, Renjiao Yi, Chenyang Zhu, Ke Zhuang, Wei Chen, and Kai Xu. Generic objects as pose probes for few-shot view synthesis. *IEEE Transactions on Circuits and Systems for Video Technology*, 2025. 1

[10] Samuel Gershman and Noah Goodman. Amortized inference in probabilistic reasoning. In *Proceedings of the annual meeting of the cognitive science society*, 2014. 5

[11] David Heckerman, Dan Geiger, and David M Chickering. Learning bayesian networks: The combination of knowledge and statistical data. *Machine learning*, 20:197–243, 1995. 4

[12] Irina Higgins, Loic Matthey, Arka Pal, Christopher Burgess,

Xavier Glorot, Matthew Botvinick, Shakir Mohamed, and Alexander Lerchner. beta-vae: Learning basic visual concepts with a constrained variational framework. In *International conference on learning representations*, 2016. 4

[13] Dong Huang, Chang-Dong Wang, Jian-Sheng Wu, Jian-Huang Lai, and Chee-Keong Kwok. Ultra-scalable spectral clustering and ensemble clustering. *IEEE Transactions on Knowledge and Data Engineering*, 32(6):1212–1226, 2019. 3

[14] Zhenyu Huang, Peng Hu, Joey Tianyi Zhou, Jiancheng Lv, and Xi Peng. Partially view-aligned clustering. *Advances in Neural Information Processing Systems*, 33:2892–2902, 2020. 2, 3, 7

[15] Jiaqi Jin, Siwei Wang, Zhibin Dong, Xinwang Liu, and En

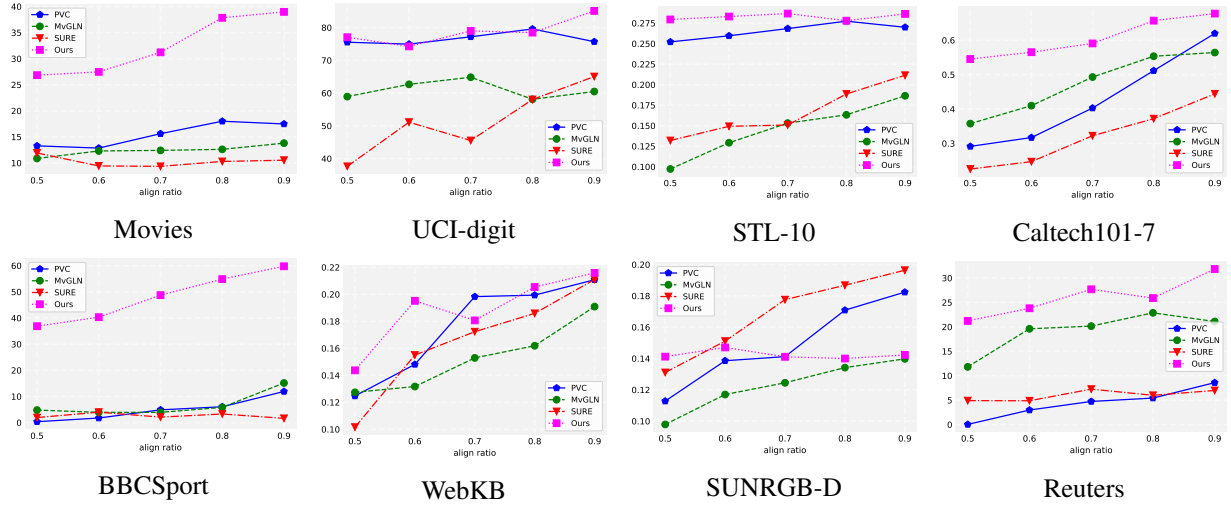


Figure 13. Clustering performance on eight Datasets with different aligned ratios in NMI metrics.

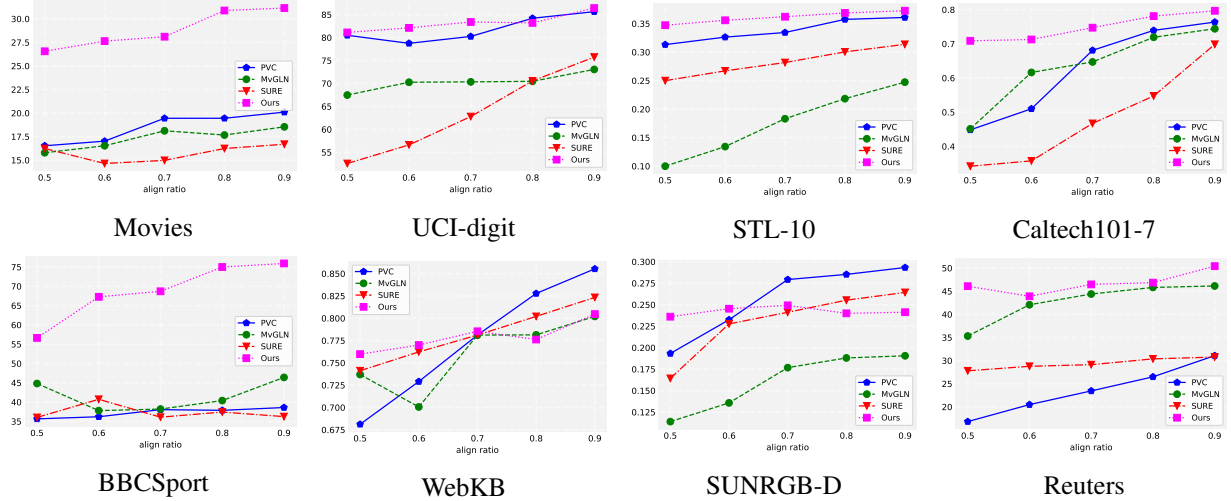


Figure 14. Clustering performance on eight Datasets with different aligned ratios in PUR metrics.

Zhu. Deep incomplete multi-view clustering with cross-view partial sample and prototype alignment. *arXiv preprint arXiv:2303.15689*, 2023. 3

- [16] Jiaqi Jin, Siwei Wang, Zhibin Dong, Xihong Yang, Xinwang Liu, En Zhu, and Kunlun He. Deep incomplete multi-view clustering with distribution dual-consistency recovery guidance. *arXiv preprint arXiv:2503.11017*, 2025. 3
- [17] Shuo Jin, Meiqin Liu, Chao Yao, Chunyu Lin, and Yao Zhao. Kernel dimension matters: To activate available kernels for real-time video super-resolution. In *Proceedings of the 31st ACM International Conference on Multimedia*, pages 8617–8625, 2023. 1
- [18] Diederik P Kingma and Jimmy Ba. Adam: A method for stochastic optimization. *arXiv preprint arXiv:1412.6980*, 2014. 7
- [19] Murat Kocaoglu, Christopher Snyder, Alexandros G Di-

makis, and Sriram Vishwanath. Causalgan: Learning causal implicit generative models with adversarial training. *arXiv preprint arXiv:1709.02023*, 2017. 4

- [20] Zhenglai Li, Chang Tang, Xinwang Liu, Xiao Zheng, Wei Zhang, and En Zhu. Consensus graph learning for multi-view clustering. *IEEE Transactions on Multimedia*, 24: 2461–2472, 2021. 3
- [21] Dawen Liang, Rahul G Krishnan, Matthew D Hoffman, and Tony Jebara. Variational autoencoders for collaborative filtering. In *Proceedings of the 2018 world wide web conference*, pages 689–698, 2018. 5, 6
- [22] Chenghua Liu, Zhuolin Liao, Yixuan Ma, and Kun Zhan. Stationary diffusion state neural estimation for multiview clustering. In *Proceedings of the AAAI Conference on Artificial Intelligence*, pages 7542–7549, 2022. 7
- [23] Meiqin Liu, Shuo Jin, Chao Yao, Chunyu Lin, and Yao

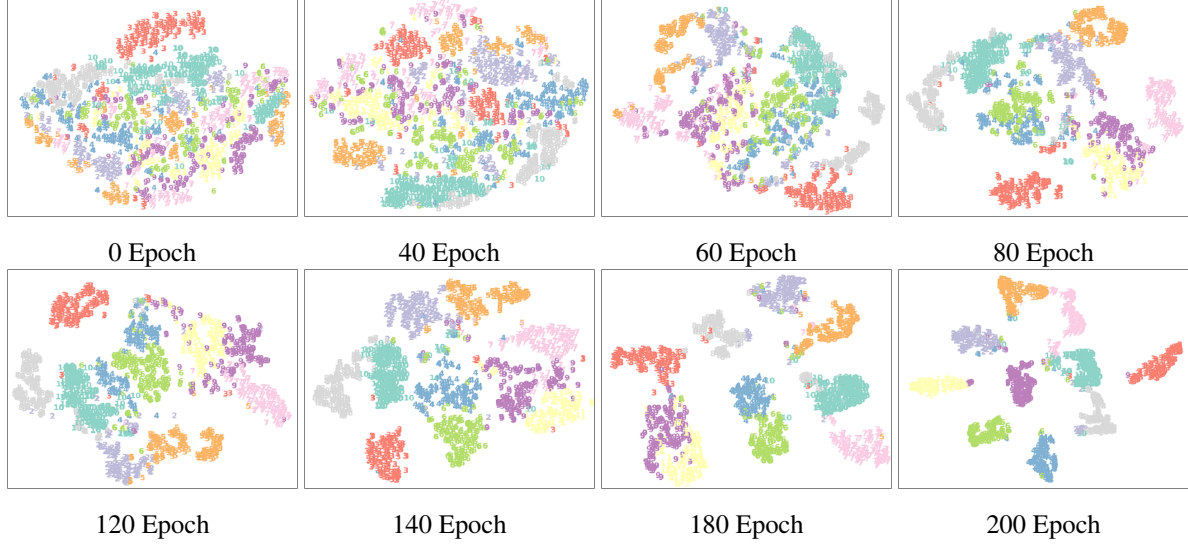


Figure 15. Visualization of the representations during the training process on UCI-digit dataset.

Zhao. Temporal consistency learning of inter-frames for video super-resolution. *IEEE Transactions on Circuits and Systems for Video Technology*, 33(4):1507–1520, 2022. 1

[24] Suyuan Liu, Siwei Wang, Pei Zhang, Kai Xu, Xinwang Liu, Changwang Zhang, and Feng Gao. Efficient one-pass multi-view subspace clustering with consensus anchors. In *Proceedings of the AAAI Conference on Artificial Intelligence*, pages 7576–7584, 2022. 3

[25] Suyuan Liu, Qing Liao, Siwei Wang, Xinwang Liu, and En Zhu. Robust and consistent anchor graph learning for multi-view clustering. *IEEE Transactions on Knowledge and Data Engineering*, 2024. 3

[26] Xinwang Liu. Simplemkmm: Simple multiple kernel k-means. *IEEE Transactions on Pattern Analysis and Machine Intelligence*, 2022. 3

[27] Xinwang Liu, Li Liu, Qing Liao, Siwei Wang, Yi Zhang, Wenxuan Tu, Chang Tang, Jiyuan Liu, and En Zhu. One pass late fusion multi-view clustering. In *International Conference on Machine Learning*, pages 6850–6859. PMLR, 2021. 3

[28] Yue Liu, Wenxuan Tu, Sihang Zhou, Xinwang Liu, Linxuan Song, Xihong Yang, and En Zhu. Deep graph clustering via dual correlation reduction. In *AAAI Conference on Artificial Intelligence*, 2022. 3

[29] Yixin Liu, Yu Zheng, Daokun Zhang, Hongxu Chen, Hao Peng, and Shirui Pan. Towards unsupervised deep graph structure learning. *arXiv preprint arXiv:2201.06367*, 2022. 7

[30] Yue Liu, Ke Liang, Jun Xia, Sihang Zhou, Xihong Yang, , Xinwang Liu, and Z. Stan Li. Dink-net: Neural clustering on large graphs. In *Proc. of ICML*, 2023. 3

[31] Yue Liu, Xihong Yang, Sihang Zhou, Xinwang Liu, Zhen Wang, Ke Liang, Wenxuan Tu, Liang Li, Jingcan Duan, and Cancan Chen. Hard sample aware network for contrastive deep graph clustering. In *Proceedings of the AAAI conference on artificial intelligence*, pages 8914–8922, 2023. 3

[32] Zhen Long, Ce Zhu, Pierre Comon, Yazhou Ren, and Yipeng Liu. Feature space recovery for efficient incomplete multi-view clustering. *IEEE Transactions on Knowledge and Data Engineering*, 2023. 3

[33] Ziwei Niu, Hongyi Wang, Hao Sun, Shuyi Ouyang, Yen-wei Chen, and Lanfen Lin. Mckd: Mutually collaborative knowledge distillation for federated domain adaptation and generalization. In *ICASSP 2023-2023 IEEE International Conference on Acoustics, Speech and Signal Processing (ICASSP)*, pages 1–5. IEEE, 2023. 3

[34] Ziwei Niu, Junkun Yuan, Xu Ma, Yingying Xu, Jing Liu, Yen-Wei Chen, Ruofeng Tong, and Lanfen Lin. Knowledge distillation-based domain-invariant representation learning for domain generalization. *IEEE Transactions on Multimedia*, 26:245–255, 2023. 3

[35] Judea Pearl. *Causality*. Cambridge university press, 2009. 4

[36] Danilo Jimenez Rezende, Shakir Mohamed, and Daan Wierstra. Stochastic backpropagation and approximate inference in deep generative models. In *International conference on machine learning*, pages 1278–1286. PMLR, 2014. 5

[37] Alexander Shapiro. Monte carlo sampling methods. *Handbooks in operations research and management science*, 10: 353–425, 2003. 6

[38] Shohei Shimizu, Patrik O Hoyer, Aapo Hyvärinen, Antti Kerminen, and Michael Jordan. A linear non-gaussian acyclic model for causal discovery. *Journal of Machine Learning Research*, 7(10), 2006. 4

[39] Yuan Sun, Yang Qin, Yongxiang Li, Dezhong Peng, Xi Peng, and Peng Hu. Robust multi-view clustering with noisy correspondence. *IEEE Transactions on Knowledge and Data Engineering*, 2024. 1, 7

[40] Raphael Suter, Djordje Miladinovic, Bernhard Schölkopf, and Stefan Bauer. Robustly disentangled causal mechanisms: Validating deep representations for interventional robustness. In *International Conference on Machine Learning*, pages 6056–6065. PMLR, 2019. 4

[41] Huayi Tang and Yong Liu. Deep safe multi-view clustering: Reducing the risk of clustering performance degradation caused by view increase. In *Proceedings of the IEEE/CVF Conference on Computer Vision and Pattern Recognition*, pages 202–211, 2022. 7

[42] Daniel J Trosten, Sigurd Lokse, Robert Jenssen, and Michael Kampffmeyer. Reconsidering representation alignment for multi-view clustering. In *Proceedings of the IEEE/CVF conference on computer vision and pattern recognition*, pages 1255–1265, 2021. 7

[43] Laurens Van der Maaten and Geoffrey Hinton. Visualizing data using t-sne. *Journal of machine learning research*, 9(11), 2008. 9

[44] Xinhang Wan, Jiyuan Liu, Weixuan Liang, Xinwang Liu, Yi Wen, and En Zhu. Continual multi-view clustering. In *Proceedings of the 30th ACM International Conference on Multimedia*, pages 3676–3684, 2022. 1, 3

[45] Xinhang Wan, Jiyuan Liu, Xinbiao Gan, Xinwang Liu, Siwei Wang, Yi Wen, Tianjiao Wan, and En Zhu. One-step multi-view clustering with diverse representation. *IEEE Transactions on Neural Networks and Learning Systems*, pages 1–13, 2024.

[46] Xinhang Wan, Bin Xiao, Xinwang Liu, Jiyuan Liu, Weixuan Liang, and En Zhu. Fast continual multi-view clustering with incomplete views. *IEEE Transactions on Image Processing*, 33:2995–3008, 2024. 1

[47] Fangdi Wang, Jiaqi Jin, Zhibin Dong, Xihong Yang, Yu Feng, Xinwang Liu, Xinzhou Zhu, Siwei Wang, Tianrui Liu, and En Zhu. View gap matters: Cross-view topology and information decoupling for multi-view clustering. In *Proceedings of the 32nd ACM International Conference on Multimedia*, pages 8431–8440, 2024. 7

[48] Tan Wang, Jianqiang Huang, Hanwang Zhang, and Qianru Sun. Visual commonsense r-cnn. In *Proceedings of the IEEE/CVF conference on computer vision and pattern recognition*, pages 10760–10770, 2020. 6

[49] Wenjie Wang, Xinyu Lin, Fuli Feng, Xiangnan He, Min Lin, and Tat-Seng Chua. Causal representation learning for out-of-distribution recommendation. In *Proceedings of the ACM Web Conference 2022*, pages 3562–3571, 2022. 5, 6

[50] Jie Wen, Zheng Zhang, Yong Xu, and Zuofeng Zhong. Incomplete multi-view clustering via graph regularized matrix factorization. In *Proceedings of the European conference on computer vision (ECCV) workshops*, pages 0–0, 2018. 3

[51] Yi Wen, Siwei Wang, Qing Liao, Weixuan Liang, Ke Liang, Xinhang Wan, and Xinwang Liu. Unpaired multi-view graph clustering with cross-view structure matching. *IEEE Transactions on Neural Networks and Learning Systems*, 2023. 3, 4

[52] Yang Xihong, Jing Heming, Zhang Zixing, Wang Jindong, Niu Huakang, Wang Shuaiqiang, Lu Yu, Wang Junfeng, Yin Dawei, Liu Xinwang, Zhu En, Lian Defu, and Min Erxue. Darec: A disentangled alignment framework for large language model and recommender system. In *2025 IEEE 41st International Conference on Data Engineering (ICDE)*. IEEE, 2025. 3

[53] Jie Xu, Yazhou Ren, Huayi Tang, Zhimeng Yang, Lili Pan, Yang Yang, Xiaorong Pu, S Yu Philip, and Lifang He. Self-supervised discriminative feature learning for deep multi-view clustering. *IEEE Transactions on Knowledge and Data Engineering*, 2022. 7

[54] Jie Xu, Huayi Tang, Yazhou Ren, Liang Peng, Xiaofeng Zhu, and Lifang He. Multi-level feature learning for contrastive multi-view clustering. In *Proceedings of the IEEE/CVF Conference on Computer Vision and Pattern Recognition*, pages 16051–16060, 2022. 1, 7

[55] Weiqing Yan, Yuanyang Zhang, Chenlei Lv, Chang Tang, Guanghui Yue, Liang Liao, and Weisi Lin. Gcfagg: Global and cross-view feature aggregation for multi-view clustering. In *Proceedings of the IEEE/CVF Conference on Computer Vision and Pattern Recognition*, pages 19863–19872, 2023. 7

[56] Mouxing Yang, Yunfan Li, Zhenyu Huang, Zitao Liu, Peng Hu, and Xi Peng. Partially view-aligned representation learning with noise-robust contrastive loss. In *Proceedings of the IEEE/CVF conference on computer vision and pattern recognition*, pages 1134–1143, 2021. 3, 7

[57] Mengyue Yang, Furui Liu, Zhitang Chen, Xinwei Shen, Jianye Hao, and Jun Wang. Causalvae: Disentangled representation learning via neural structural causal models. In *Proceedings of the IEEE/CVF conference on computer vision and pattern recognition*, pages 9593–9602, 2021. 5

[58] Mouxing Yang, Yunfan Li, Peng Hu, Jinfeng Bai, Jiancheng Lv, and Xi Peng. Robust multi-view clustering with incomplete information. *IEEE Transactions on Pattern Analysis and Machine Intelligence*, 45(1):1055–1069, 2022. 2, 3, 4, 7

[59] Xihong Yang, Xiaochang Hu, Sihang Zhou, Xinwang Liu, and En Zhu. Interpolation-based contrastive learning for few-label semi-supervised learning. *IEEE Transactions on Neural Networks and Learning Systems*, pages 1–12, 2022. 3

[60] Xihong Yang, Jiaqi Jin, Siwei Wang, Ke Liang, Yue Liu, Yi Wen, Suyuan Liu, Sihang Zhou, Xinwang Liu, and En Zhu. Dealmvic: Dual contrastive calibration for multi-view clustering. In *Proceedings of the 31th ACM International Conference on Multimedia*, 2023. 1, 3, 6, 7

[61] Xihong Yang, Yue Liu, Sihang Zhou, Siwei Wang, Wenxuan Tu, Qun Zheng, Xinwang Liu, Liming Fang, and En Zhu. Cluster-guided contrastive graph clustering network. In *Proceedings of the AAAI conference on artificial intelligence*, pages 10834–10842, 2023. 3, 7

[62] Xihong Yang, Cheng Tan, Yue Liu, Ke Liang, Siwei Wang, Sihang Zhou, Jun Xia, Stan Z Li, Xinwang Liu, and En Zhu. Convert: Contrastive graph clustering with reliable augmentation. In *Proceedings of the 31st ACM International Conference on Multimedia*, pages 319–327, 2023. 7

[63] Xihong Yang, Erxue Min, Ke Liang, Yue Liu, Siwei Wang, Sihang Zhou, Huijun Wu, Xinwang Liu, and En Zhu. Graphlearner: Graph node clustering with fully learnable augmentation. In *Proceedings of the 32nd ACM International Conference on Multimedia*, pages 5517–5526, 2024.

[64] Xihong Yang, Yiqi Wang, Yue Liu, Yi Wen, Lingyuan Meng, Sihang Zhou, Xinwang Liu, and En Zhu. Mixed graph contrastive network for semi-supervised node classification. *ACM Transactions on Knowledge Discovery from Data*, 2024. 3, 7

[65] Xihong Yang, Siwei Wang, Fangdi Wang, Jiaqi Jin, Suyuan Liu, Yue Liu, En Zhu, Xinwang Liu, and Yueming Jin. Automatically identify and rectify: Robust deep contrastive multi-view clustering in noisy scenarios. In *International Conference on Machine Learning*. PMLR, 2025. 1, 3

[66] Xihong Yang, Yiqi Wang, Jin Chen, Wenqi Fan, Xiangyu Zhao, En Zhu, Xinwang Liu, and Defu Lian. Dual test-time training for out-of-distribution recommender system. *IEEE Transactions on Knowledge and Data Engineering*, 37(6):3312–3326, 2025. 3

[67] Mingjia Yin, Hao Wang, Wei Guo, Yong Liu, Suojuan Zhang, Sirui Zhao, Defu Lian, and Enhong Chen. Dataset regeneration for sequential recommendation. In *Proceedings of the 30th ACM SIGKDD Conference on Knowledge Discovery and Data Mining*, pages 3954–3965, 2024. 3

[68] Hong Yu, Jia Tang, Guoyin Wang, and Xinbo Gao. A novel multi-view clustering method for unknown mapping relationships between cross-view samples. In *Proceedings of the 27th ACM SIGKDD Conference on Knowledge Discovery & Data Mining*, pages 2075–2083, 2021. 2, 4, 7

[69] Shengju Yu, Zhibing Dong, Siwei Wang, Xinhang Wan, Yue Liu, Weixuan Liang, Pei Zhang, Wenxuan Tu, and Xinwang Liu. Towards resource-friendly, extensible and stable incomplete multi-view clustering. In *Proceedings of the 41st International Conference on Machine Learning*, pages 57415–57440, 2024. 1

[70] Shengju Yu, Siwei Wang, Zhibin Dong, Wenxuan Tu, Suyuan Liu, Zhao Lv, Pan Li, Miao Wang, and En Zhu. A non-parametric graph clustering framework for multi-view data. In *Proceedings of the AAAI conference on artificial intelligence*, pages 16558–16567, 2024.

[71] Shengju Yu, Suyuan Liu, Siwei Wang, Chang Tang, Zhigang Luo, Xinwang Liu, and En Zhu. Sparse low-rank multi-view subspace clustering with consensus anchors and unified bipartite graph. *IEEE Transactions on Neural Networks and Learning Systems*, 36(1):1438–1452, 2025. 1

[72] Yang Zhang, Yufei Wang, Quan Z Sheng, Adnan Mahmood, Wei Emma Zhang, and Rongying Zhao. Tdm-cfc: Towards document-level multi-label citation function classification. In *International Conference on Web Information Systems Engineering*, pages 363–376. Springer, 2021. 3

[73] Yang Zhang, Rongying Zhao, Yufei Wang, Haihua Chen, Adnan Mahmood, Munazza Zaib, Wei Emma Zhang, and Quan Z Sheng. Towards employing native information in citation function classification. *Scientometrics*, 127(11):6557–6577, 2022.

[74] Yang Zhang, Yufei Wang, Kai Wang, Quan Z Sheng, Lina Yao, Adnan Mahmood, Wei Emma Zhang, and Rongying Zhao. When large language models meet citation: A survey. *arXiv preprint arXiv:2309.09727*, 2023. 3

[75] Qun Zheng, Xihong Yang, Siwei Wang, Xinru An, and Qi Liu. Asymmetric double-winged multi-view clustering network for exploring diverse and consistent information. *Neural Networks*, 179:106563, 2024. 1, 3

[76] Xun Zheng, Bryon Aragam, Pradeep K Ravikumar, and Eric P Xing. Dags with no tears: Continuous optimization for structure learning. *Advances in neural information processing systems*, 31, 2018. 4